NEOPLASIA
www.neoplasia.com
Volume 21 Number 12 December 2019 pp. 1121–1132

Original Research

PODXL1 promotes metastasis of the pancreatic ductal adenocarcinoma by activating the C5aR/C5a axis from the tumor microenvironment

Ken Saito[a]; Hidekazu Iioka[a]; Satoshi Maruyama[b]; I. Wayan Sumardika[c]; Masakiyo Sakaguchi[c]; Eisaku Kondo[a,*]

[a]Division of Molecular and Cellular Pathology, Niigata University Graduate School of Medical and Dental Sciences, 757 Ichibancho, Asahimachi-dori, Chuo Ward, Niigata City 951-8510, Japan; [b]Oral Pathology Section, Department of Surgical Pathology, Niigata University Hospital, 2-5274 Gakkoucho-dori, Chuo Ward, Niigata City 951-8514, Japan; [c]Department of Cell Biology, Okayama University Graduate School of Medicine, Dentistry and Pharmaceutical Sciences, 2-5-1 Shikata-cho, Kita-ku, Okayama 700-8558 Japan

Abstract

Pancreatic invasive ductal adenocarcinoma (PDAC) is a representative intractable malignancy under the current cancer therapies, and is considered a scirrhous carcinoma because it develops dense stroma. Both *PODXL1*, a member of CD34 family molecules, and C5aR, a critical cell motility inducer, have gained recent attention, as their expression was reported to correlate with poor prognosis for patients with diverse origins including PDAC; however, previous studies reported independently on their respective biological significance. Here we demonstrate that *PODXL1* is essential for metastasis of PDAC cells through its specific interaction with C5aR. *In vitro* assay demonstrated that PODXL1 bound to C5aR, which stabilized C5aR protein and recruited it to cancer cell plasma membranes to receive C5a, an inflammatory chemoattractant factor. *PODXL1* knockout in PDAC cells abrogated their metastatic property *in vivo*, emulating the liver metastatic mouse model treated with antiC5a neutralizing antibody. In molecular studies, PODXL1 triggered EMT on PDAC cells in response to stimulation by C5a, corroborating PODXL1 involvement in PDAC cellular invasive properties via specific interaction with the C5aR/C5a axis. Confirming the molecular assays, histological examination showed coexpression of PODXL1 and C5aR at the invasive front of primary cancer nests as well as in liver metastatic foci of PDAC both in the mouse metastasis model and patient tissues. Hence, the novel direct interaction between PODXL1 and the C5aR/C5a axis may provide a better integrated understanding of PDAC biological characteristics including its tumor microenvironment factors.

Neoplastic (2019) 21 1121–1132

Introduction

Invasive ductal adenocarcinoma of the pancreas (PDAC) is the most common pancreatic malignancy and has been recently highlighted as a serious issue for cancer treatment, given persistent clinical intractability to known therapeutic countermeasures aimed at improving patient prognosis [1,2]. PDAC shows unique histology, where proliferating cancer nests are surrounded by abundant collagenous stroma with cancerassociated fibroblasts (CAFs), inflammatory cells such as macro-

Abbreviations: PODXL1, Podocalyxinlike 1, PDAC, pancreatic invasive ductal adenocarcinoma, C5aR, Complement component 5a receptor 1 (C5aR1, CD88), CAF, cancerassociated fibroblast, EMT, epithelialmesenchymal transition, iPS, induced pluripotent stem, ITGB1, Integrin 1, WT, wild type, KO, knockout, IHC, immunohistochemistry, IB, immunoblot, IP, immunoprecipitation, IF, immunofluorescence, HPNE, human immortalized pancreatic ductal epithelium, NHDF, normal human dermal fibroblast, MMP, matrix metalloproteinases, Ab, antibody

Corresponding author at: Division of Molecular and Cellular Pathology, Niigata University Graduate School of Medical and Dental Sciences, 757 Ichibancho, Asahimachi-dori, Chuo Ward, Niigata City 951-8510, Japan.
e-mail address: ekondo@med.niigata-u.ac.jp (E. Kondo).

Received 29 May 2019; received in revised form 17 September 2019; accepted 18 September 2019

https://doi.org/10.1016/j.neo.2019.09.003

phages and lymphocytes, and scanty tumor blood vessels from neovascularization. These stromal components form a so called tumor microenvironment essential to cancer progression *in vivo*. Hence, tumor microenvironments are complex systems of various cellular components, observed to release diverse inflammatory chemokines that interact with cancer cells resulting in tumor growth, invasion and metastasis.

Podocalyxinlike 1 (*PODXL1*), is an antiadhesive sialomucin, belonging to a member of the CD34 family harboring the extracellular domain and intracellular domain via the transmembrane portion. It is expressed by normal vascular endothelium, renal podocyte, and hematopoietic progenitors [3–5] and has been reported to be a stem cell marker including embryonic stem cells [6,7]. Noticeably, there have been studies demonstrating correlation between PODXL1 expression and poor prognosis of patients with cancer of the diverse origins including colorectal cancer [8], gastric cancer [9], and pancreatic cancer [10]. Functionally, PODXL1 was reported to promote invadepodia formation and metastasis through Rac1/Cdc42/cortactin signaling in breast cancer cells [11], to induce collective migration of MCF7 cells depending on activity of the actin scaffolding cytoplasmic protein ezrin [12]. Recently, it was revealed that PODXL1 was involved in efficient EMT extravasating via the Ezrin signaling on breast cancer and pancreatic cancer cells [13]. Hence, PODXL1 appears critically involved in causing invasion and metastasis of various cancers and is one of the most important regulators of human malignancies; however, the diverse biological roles of PODXL1 still require elucidation for generating future cancer therapeutics. On the other hand, multiple chemokines have been reported as produced in tumor microenvironment in response to inflammatory reaction and tumor immunity against cancer cells. Among them, C5a, a soluble complement which is related to inflammatory reaction and chemotactic response, has been reported to promote tumor development and progression including cellular motility and invasion, and its expression was related to poor prognosis in PDAC patients, on account of interaction with Gproteincoupled complement receptor, C5a receptor (C5aR; CD88) [14–17]. Thus the C5aC5aR interaction in cancer stroma has been recently highlighted as a key accelerator of cancer metastasis in tumors with diverse origins, such as breast, lung and gastric cancers [14–17].

Here, we demonstrated the novel function of PODXL1 capture of a key metastatic regulator, C5aR, in the PDAC microenvironment, to stabilize and activate it as specific binding partner, triggering PDAC invasion and metastasis by accelerating tumor cell motility through activation of the C5aR/C5a axis.

Materials and methods

Cell culture and antibodies

Human PDAC lines, BxPC3 (ATCC: CRL1687), AsPC1 (ATCC: CRL1682), MiaPaCa2 (ATCC: CRMCRL1420), Panc1 (ATCC: CRL1469), an immortalized nonneopastic pancreatic ductal cell, HPNE (ATCC: CRL4023), normal human dermal fibroblast, NHDF (ATCC: PCS201010) were grown in RPMI1640 (Wako, Tokyo, Japan) supplemented with 10% of fetal bovine serum (FBS) in a 5% CO_2 incubator. Authentication of each cell line was attached. Antibodies employed in this study were as follows. As a primary antibody, antiPODXL1 (SigmaAldrich, Merk, St. Louis, MO), antiIntegrin 1 (Invitrogen, Thermo Fisher Scientific KK, Japan), antiC5aR (CD88) (Hycult Biotech, Wayne, PA), antiC5a (R&D Systems, Mineapollice, MN), antiMyctag (SigmaAldrich), antiFLAGtag (Invitrogen, Thermo Fisher Scientific KK), antiTubulin (CST Japan, Tokyo, Japan), antiECadherin (Invitrogen, Thermo Fisher Scientific KK), antiSnail (CST Japan), antiVimentin (CST Japan), antiTRA160 (CST Japan). As a secondary antibody, Alexa488conjugated goat antimouse IgG(H + L), Alexa488goat antimouse IgM, Alexa555goat antimouse IgG(H + L), Alexa488goat antirabbit IgG(H + L), Alexa555goat antirabbit IgG(H + L), Alexa555donkey antigoat IgG(H + L), HRPconjugated goat antimouse IgG(H + L), HRPgoat antirabbit IgG(H + L) (for all of these: Invitrogen, Thermo Fisher Scientific KK) were used for the immunohistochemistry, immunofluorescence and immunoblot assays.

Patients tissues, immunohistochemistry and immunofluorescence

Paraffinembedded surgical specimens fixed with 10% bufferedformalin and made from the patient tissues of the pancreatic invasive ductal adenocarcinoma were obtained from the department of pathology, Niigata Cancer Center Hospital under approval by the ethics committees of Niigata University and Niigata Cancer Center. Ten cases of primary PDAC tissues (well differentiated; 3 cases, moderately differentiated; 4 case, poorly differentiated; 3 cases) and four cases of liver metastasis of the corresponding PDAC from the same individual among these ten patients were examined for expression for the proteins of the interest by immunohistochemistry and immunofluorescence, using antiPODXL1, antiC5aR, and antiC5a, antiTRA160 antibodies. All specimens were autoclaved prior to incubation with the primary antibody (at 4 celcius for 12hours) for immunohistochemistry or immunofluorescence.

Plasmid construction for a panel assay of the chemokine receptors

For the panel screening of chemokine receptors as a binding partner of PODXL1, the plasmids encoding, in total, forty human chemokine receptor were constructed, respectively. These were contransfected with human *PODXL1* and subjected to immunoprecipitation assay. In detail, for the expressor plasmid construction, cDNAs of interest were subcloned into the pIDTSMART (CTSC) vector to obtain efficient gene expression in a transient manner [18]. The prepared cDNAs covering the entire ORF were as follows: human cDNAs encoding *PODXL1* (transcript variant 1; GenBank NM_001018111) and chemokine receptors (*C3aR, C5aR, CXCR16, CX3CR1, XCR1, CCR111, BLT1, 2, LTR1,2, EP14, DP1,2, FP, IP, TP,* and *LPAR16*). *PODXL1* was designed to express as a Cterminal 3xMyc6xHistagged form. Chemokine receptors were all designed to express as Cterminal 3xFlag6xHistagged forms.

Immunoblot and immunoprecipitation

All immunoblot analyses were performed with the cell lysates prepared with MPER mammalian protein extraction reagent (Thermo Fisher Scientific) under standard conditions using each of the specific antibodies mentioned above. For the coimmunoprecipitation assay, HEK293T cells were transiently transfected with the *PODXL1* expressor (*PODXL1* with 3xMyc6xHistagged at the Cterminal end). Chemokine receptors were all designed to express as Cterminal 3xFlag6xHistagged forms. Combined with a series of chemokine receptorexpressors mentioned above using FuGENEHD (Promega), respectively. Twentyfour hours postcotransfection, cell pellets were harvested and lysed in MPER buffer. The prepared lysates were then incubated with agarose beads conjugated with monoclonal antiMyc tag antibody (MBL, Nagoya, Japan). The resultant immunoprecipitates were subjected to immunoblot probed with antiFlag tag antibody. To examine direct binding between PODXL1 and C5aR, PODXL1 was purified from the cell lysate of the *PODXL1*-HA(x3)His(x6)tagged expressortransfected HEK293T cells using antiHistag antibodyconjugated beads (#D2918; antiHistag mABagarose beads; MBL Co. Ltd., Japan). C5aR protein was also isolated from the lysate of the *C5aR*Flag(x3)His(x6)tagged expressortransfected 293 T cells using antiHistag mAb beads. Each protein was mixed together, incubated for 30 min at RT, then the sample was precipitated using beads conju-

gated with antiHAtag antibody (#5618; antiHAtag pAbagarose beads; MBL Co. Ltd., Japan) for pulldown of PODXL1. The pulldown sample was subjected to SDSPAGE, blotted onto membrane after fractioned, and immunoblotting with antiHA antibody (#3724; HATag C29F4; Cell Signaling Technology, Danvers, MA) or with antiFlag antibody (#F1804; antiFlag M2 mAb; Sigma Aldrich Japan, Tokyo, Japan) was performed, respectively. As a control, purified PODXL1HAHis alone and PODXL1HAHis incubated with heatdegraded C5aRFlagHis protein were employed.

Generation of PODXL1′ clones by the CRISPR/Cas9 system

*PODXL1*knockout PDAC cell lines (for MIaPaCa2, AsPC1, and Panc1) were generated using CRISPR/Cas9 system. Both plasmids, hCas9 (#41815 Addgene, Watertown, MA), and gRNA (guide RNA) Cloning Vector (#41824), were obtained from Addgene. The gRNA vector including *PODXL1* target sequence (CGACACGATGCGCTGCGCGCtgg) located in part of the Exon 1 was prepared following the manufacturers instruction with tgg sequence as a Protospacer Adjacent Motif (PAM). The hCas9 and *PODXL1* gRNA vector were cotransfected into cells using ViaFect Transfection Reagent (#E4981, Promega, Madison, WI). Twentyfour hours posttransfection, the cells were cultured with RPMI medium containing 500 g/ml of Geneticin (#1013135, Gibco, Thermo Fisher Scientific, Waltham, MA) for isolating the Geneticinresistant clones. PODXL1expression deficient clones from each PDAC line were confirmed by lack of PODXL1 protein, using immunoblot analysis with antiPODXL1 antibody. Genetic mutation of *PODXL1* in the knockout clone was also examined by genomic DNA sequencing of PCRamplified product, using the specific primers for *PODXL1*target sequence and the adjacent genomic DNA. The primers used for the sequencing were the following: Pod1.Ex1.check.Fw2: 5CAGCGGCAGGGAGGAAGAGC and Pod1.Ex1.check.Rv2 5GCGGTGCGGTCTCCCTTTTCTT.

Image based protein–protein interaction (PPI) analysis (Fluoppi assay)

The proteinprotein interaction between PODXL1 and candidate proteins (EP4, CXCR2, C5AR, LTB4R, CTTN and CXCR1) was detected using the FluoPPI system (MBL, Nagoya, Japan), in which PPIs were visualized as fluorescent foci [19,20]. *PODXL1* was subcloned into a pAshMNL ver.2 plasmid to fuse with an Ash (homo oligomerized protein assembly helper) tag (*PODXL1*Ash). Candidates were subcloned into a pMontiRedMNL plasmid to fuse with a MontiRed (homo tetramer red fluorescent protein from Montipora sp.) tag (*CTNN*red or *C5aR*red). These plasmids of *PODXL1*Ash and candidatesRed were cotransfected into HeLa cells using Lipofectamine 3000 (Thermo Fisher Scientific, Waltham, MA, USA) according to the manufacturers instructions, respectively, and intracellular fluorescent foci with red color were observed by inverted fluorescence microscope (Olympus IX71, Olympus Co. Tokyo, Japan) and detected as an image using cellSens imaging software (Olympus Co.).

Invasion assay

Cells were starved by serum free medium for 24 h prior to invasion and migration assays. Cell invasion and migration assays were both evaluated by the Boyden chamber method using the filter inserts (pore size, 8 m), precoated (for invasion assay) or not precoated (for migration assay) with Matrigel in 24well plates (BD Biosciences, Franklin Lakes, NJ, USA). Each pancreatic cancer cell line (7.5 10^4 cells/insert for MIA PaCa2, 2 10^5 cells/insert for AsPC1, or 4 10^4 cells/insert for PANC1) was seeded on the top chamber. The top chamber was filled with serumfree medium and the bottom chamber was filled with 10% FBS medium. The recombinant chemokines were then set in the bottom chamber at a final concentration of 25 ng/ml for CXCL8 (PeproTech, Rocky Hill, NJ, USA), and 0.5 M for PGE2, 5 ng/mL for CX3CL1 (R&D Systems, Minneapolis, MN, USA) and C5a (ProSpecTany Technology Ltd, Ness Ziona, Israel). After incubation for 8 h in the case of PANC1, or 48 h in the case of MIA PaCa2 and AsPC1cells, cells that passed through the filter and were attached to the lower surface of the filter were counted by staining with 0.01% crystal violet in 25% methanol. Cells attached to the lower surface of the filter membrane were then quantified by cell counting in five nonoverlapping fields at 100 magnification.

RNA interference assay using siRNA

Predesigned siRNAs for human *C5aR* (ID D00544200005) and control siRNA (ID D0018101005) were purchased from Dharmacon (Lafayette, Colorado, USA). siRNAs (final concentration 50 nM) were transfected using Lipofectamin RNAiMAX reagent (Thermo Fisher Scientific). Fortyeight hours postintroduction of each siRNA, the cells were subjected to the invasion assay described above.

In vivo mouse liver metastasis model

1 10^6 cells of MiaPaCa2, AsPC1, or Panc1 were injected into 6 weekold nude mouse spleen exteriorized through a left flank incision, respectively, followed by splenectomy 2 min later. The same number of the *PODXL1′* PDAC cells corresponding to each cell line were injected in the same way with the same timing. Approximately 30 days postinjection, the mice grew metastatic liver tumors derived from the injected PDAC cells, and they were then autopsied and compared for tumor formation pairwise with the mice implanted with *PODXL1′* cells under the stereo microscope. Total number of mice examined in each group was four (n = 4). Only in the case of Panc1 splenic xenograft, number of mouse examined was two (n = 2). In the C5a blocking assay, each mouse with splenic injection of 1 10^6 of MiaPaCa2 cells was treated with intravenously administrated 50 g/mouse of antiC5a neutralizing antibody on Day 0 (the day of cellimplant), Day 7, Day 14 (in total three times, and once every week), and autopsied and examined on Day 30 pairwise with mice (control group) treated with the same dose of goatIgG. Totally, four mice (n = 4) were examined in each group. Excised tumors in all animal experiments were histologically examined with paraffinembedded specimens by HE staining and immunohistochemistry using antihuman cytokeratin, CAM5.2 (BD Biosciences, San Jose, CA) to demonstrate human PDAC cells (MiaPaCa2, AsPC1, and Panc1, respectively) origin.

Statistical analysis of metastatic tumors in mouse models

Based on macroscopic finding in combination with microscopic examination of the tissue specimens, number of liver metastasis was counted in each group of mouse splenically injected with MiaPaCa2, AsPC1 in every animal experiment. Average number of metastasis per liver in each case was statistically evaluated by *t*test (shown as graph with *P* value).

Results

Characteristic expression of PODXL1 on human PDAC tissues

PODXL1 expression on PDAC tissues has been reported in previous studies that demonstrated PODXL1 preferentially expressed on the cancer nests in comparison with the nonneoplastic pancreatic acinus and duct, with the expression correlating to the patients poor prognosis [21]. Immunohistochemistry on representative primary PDAC patient tissues using antiPODXL1 antibody revealed that strong membranous PODXL1

expression with or without cytoplasmic expression was observed mainly at the small collective cell formingcancer nests at the invasive front of the PDAC tumor in examined cases (1; well differentiated type, 2,3; moderately differentiated type, 4; poorly differentiated type, respectively) (Figure 1A), but a small number of strong PODXL1positive cancer cells were observed among the individual tumor glands adjacent to the small invasive nests (Supplementary Figure S1A). PODXL1 expression was not dependent on the differentiation type of PDAC but was detected in all types examined. It has been also reported that the glycosylated form of PODXL1 was recognized as TRA160 antigen [22], an embryonic stem cell and iPS cell marker. TRA160 expression was detected in similar patterns to that of PODXL1, where TRA160 was strongly positive in small cancer nests at invasive foci in PDAC patient tissues under immunohistochemistry (Supplementary Figure S1B, upper panel) Immunofluorescence using antiPODXL1 and antiITGB1 (Integrin 1, CD29) antibodies highlighted the budding tumor cell from the neoplastic gland acquiring strong expression of PODXL1 as well as ITGB1, indicating PODXL1 might be required for epithelialmesenchymal transition (EMT) of the PDAC cells (Figure 1B and Supplementary Figure S1B, lower panel). Accordingly, the budding single PDAC cell was also detected by immunofluorescence using TRA160 antibody (Supplementary Figure S1B, lower panel). The robust expression of PODXL1 was also observed not only in PDAC but also various cancers, as for example, its expression on invasive nests of colorectal tubular adenocarcinomas (Supplementary Figure S1C).

PODXL1 is critically involved in metastasis of PDAC cells in vivo

To elucidate the biological role of PODXL1 in PDAC cells *in vivo*, generation of PODXL1targeted PDAC cell clones was achieved by using the CRISPR/Cas9 genome editing system. First, endogenous expression of PODXL1 was examined in four different human PDAC lines established from different patients. As nonneoplastic counterparts, human immortalized pancreatic ductal epithelium (HPNE) and normal kidney epithelial cells were also examined for its expression. Consequently, all four PDAC lines showed strong expression of PODXL1 including the supershifted (hyperglycosylated) form (Figure 2A), and HPNE showed comparably weak PODXL1 expression with a similar pattern, but the glycosylated form was not detected in kidney cells (Figure 2A). These PDAC lines showed membranous expression of PODXL1 as well as its cytoplasmic expression (Figure 2B, upper panel), representing lamellipodia and plasma membrane localization in AsPC1 and MiaPaCa2 cells (Figure 2B, lower panel). Based on this finding, genome editing to knockout *PODXL1,* including variant 1 and 2, was performed using the CRISPR/Cas9 system with the designed guideRNA (gRNA) recognizing the part of the exon 1 both on MiaPaCa2 and AsPC1, respectively (Figure 2C, left panel). Four respective *PODXL1*$^{-/-}$ (*PODXL1*KO) clones were obtained both in MiaPaCa2 (clone #3, 9, 15, 37) and AsPC1 (clone #2, 3, 9, 13), all of which were confirmed as to specific impairment of PODXL1, utilizing immunoblots and genome sequencing (Figure 2C, right panel and Supplementary Figure S2A). Using these knockout (KO) clones, the murine pancreatic tumor model of liver metastases was established by hemispleen injection of the MiaPaCa2 cells lacking PODXL1 expression (KO clone #9) and AsPC1 *PODXL*1KO cells (KO clone #2), and by using the wild type MiaPaCa2 and AsPC1 cells for comparison, respectively. After 30 days postinjection, the wild type MiaPaCa2implanted mice developed multiple metastatic foci in the liver, whereas no metastatic foci were observed in the mice implanted with the *PODXL1*KO #9 clone (Figure 2D, upper panel). Similarly, loss of liver metastasis was observed in mice injected with the AsPC1 *PODXL1*KO #2 clone in contrast to the cases with the wild type cell injection (Figure 2D, lower panel). Number of the intrahepatic metastasis per liver between group of implanted PDAC cells bearing *PODXL1* wild type and those of *PODXL1*knockout (n = 4 in each group) was summarized in graph which showed statistical significance (Figure 2D). Similarly, loss of mesenteric lymph nodal metastasis was also observed in the mice treated with the KO clone of MiaPaCa2 (n = 4 in each group, Supplementary Figure S2B), and the *PODXL1*KO clone of Panc1 PDAC cell showed the similar phenomenon (Supplementary Figure S2C). Histological examination of the intrahepatic and lymph nodal metastatic tumors demonstrated that metastatic tumors were derived from hemisplenically injected human PDAC cells in the mice treated with tumor cells bearing *PODXL1* wild type, and no micrometastatic lesion was observed even microscopically in the liver of the mice injected with tumor cells harboring *PODXL1*knockout (Supplementary Figure S3A, 3B, and 3C).

PODXL1 captures diverse chemokine receptors including C5aR

The next issue determined was how PODXL1 is critically involved in PDAC invasion/metastasis. Recently, the tumor microenvironment has received much attention because many current studies reveal its significant impact on cancer progression in terms of tumor growth, invasion and metastasis. The tumor microenvironment is a complex system comprised of fibrous stroma, tumor angiogenesis, tumor immunity and inflammatory reaction. Among these, we focused on chemokine receptors which affect the chemotactic cellular motility through interaction with soluble inflammatory chemotactic ligands in the tumor microenvironment. A panel screening for over forty chemokines was performed to find the specific association between PODXL1 and these molecules by employing immunoprecipitation. The results showed that PODXL1 bound multiple chemokine receptors such as C5aR (C5aR1), CXCR1, CXCR2, CXCR3, CXCR4, CXCR6, CX3CR1, CCR1, CCR3, CCR8, CCR9, BLT1, BLT2, EP2, EP4, DP1, DP2, FP, IP, LPAR1, LPAR2, LPAR4, LPAR5, and LPAR6 (Figure 3A). Among these, we further examined expression of selected chemokine genes semiquantitatively by RTPCR, which revealed enhanced coupling to PODXL1. Essentially all selected chemokines were more or less expressed on PDAC cells and C5aR receptor was the strongest and most consistently expressed on them (Figure 3B). Prominent membranous C5aR expression was detected on all five representative PDAC lines, BxPC3, PK8, Panc1, MiaPaCa2, and AsPC1 (Figure 3C).

PODXL1 accelerates cellular motility by regulating functional localization and stabilizing C5aR, and triggers EMT via the C5aR/C5a axis on PDAC cells

Based on these results, the biological role for protein coupling of PODXL1 and C5aR was investigated on PDAC cells bearing the wild type *PODXL1,* compared with the *PODXL1*KO cells. Confirmed specific binding of PODXL1 to C5aR was observed only in wild type *PODXL1* (*PODXL1*WT) MIaPaCa2 cells but not in the PODXL1KO cells (Figure 4A); intracellular localization of C5aR was examined with or without PODXL1 as to whether or not this would be affected by the presence of PODXL1. In image based protein–protein interaction (PPI) analysis, the so called Fluoppi system, aggregated fluorescent dots appears only when two proteins of the interest directly binds to each other. Based on the result of Fluoppi analysis using HeLa cells, C5aR was successfully recruited to lamellipodia at the cell membrane on the *PODXL1*-cotransfected cells which was recognized as aggregated red dots, as in the case of *Cortactin* (*CTNN*)*PODXL1* cotransfected cells (Figure 4B and Supplementary Figure S4A). On the other hand, it was still retained at the cytoplasm without PODXL1 expression (only with pAsh) (Figure 4B). Other chemokine receptors, such as EP4 and CX3CR1 seen as candidate binding partner to PODXL1, also displayed changes in intracellular localization to their functional site in the presence of PODXL1 (Supplementary Figure S4B). Thus, PODXL1 appeared essential for targeting

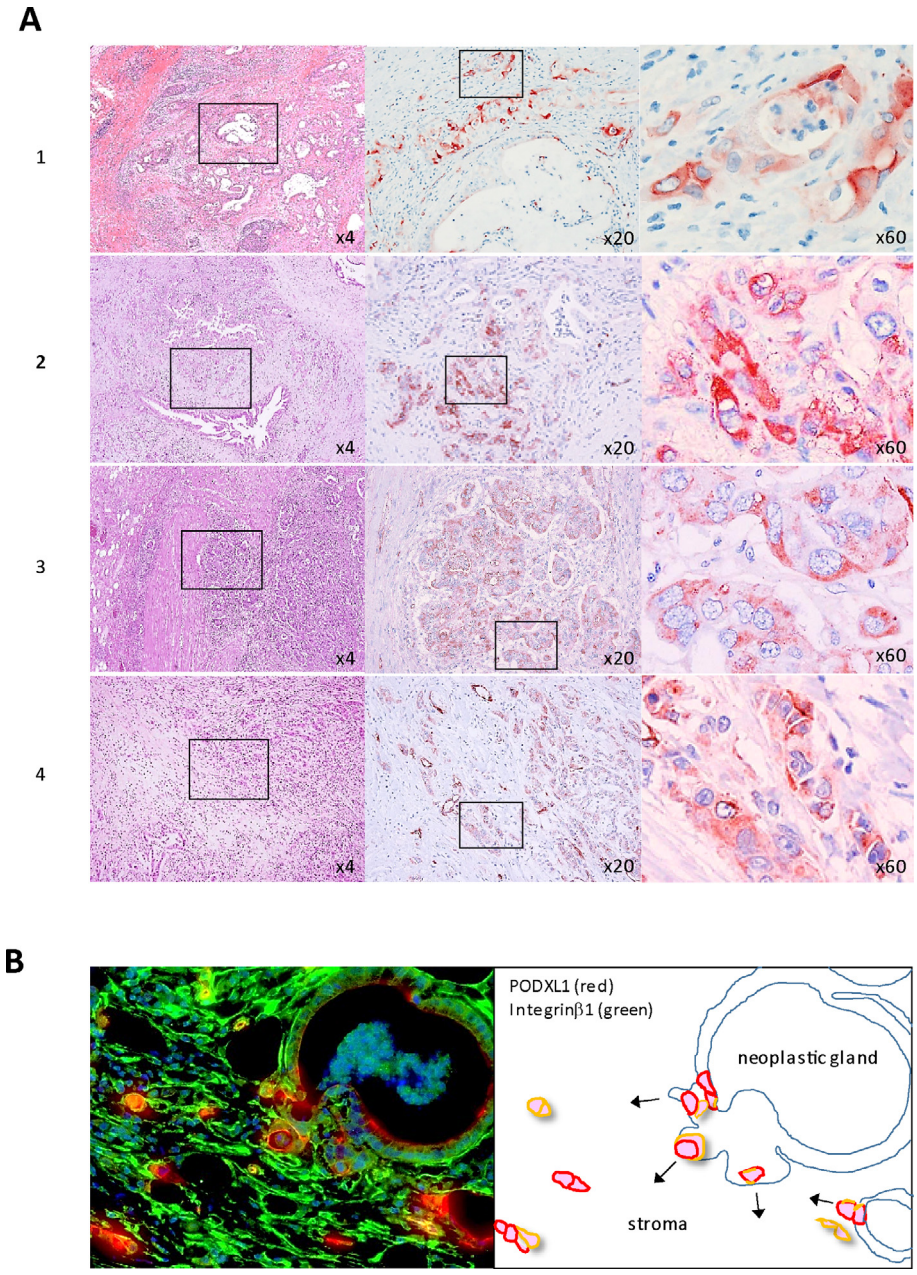

Figure 1. Expression of PODXL1 on human PDAC tissues from the patients. (A) IHC using anti-PODXL1 Ab on well differentiated type (1), moderately differentiated type (2, 3), and poorly differentiated type PDAC (4). Hatched box indicates the area for hyperview in each case (4, 20, 60). (B) Double IF using anti-PODXL1 Ab (red) and ITGB1 (green) (left panel). Schematic representation of the PODXL1-expressing budding cancer cells from the tumor gland were highlighted.

C5aR to its functional site by cellular assay. Direct coupling between PODXL1 and C5aR was also demonstrated by pulldown assay using antiHAconjugated beads to isolate binding partner of 3xHA6xHistagged PODXL1 protein (Supplementary Figure S4C). Based on the immunoprecipitation assay results – establishing the diverse chemokine receptors as binding partner with PODXL1 – CXCL8 (ligand to CXCR2), CX3CL1 (ligand to CX3CR1), C5a (ligand to C5aR), and PEG2 (ligand to EP4), all of which showed augmented association, were incubated with MiaPaCa2 cells and quantified for the increase in cellular motility, using transwellchamber assay (Boyden chamber assay), between the *PODXL1*-WT and the *PODXL1*KO cells. The data indicated that the ligand stimulation by C5a robustly increased *PODXL1*WT MiaPaCa2 cellular motility in comparison with that of C5astimulated *PODXL1*KO clone (Figure 4C). This phenomenon was specific because the MiaPaCa2 cells treated with *C5aR* siRNA markedly decreased the cellular motility even when incubating with C5a (Supplementary Figure S4A). The response to C5a seemed to be common to the other PDAC cells such as AsPC1 and Panc1 (Supplementary Figure S4B). We found that another feature of PODXL1C5aR interaction was the pronounced attenuation of C5aR expression in the *PODXL1*KO PDAC cells. In the immunofluorescence results, C5aR expression was much weaker in *PODXL1*KO MiaPaCa2 and AsPC1 in contrast to the PODXL1WT cells, and we made similar observations for *PODXL1*deficient Panc1 cells (Figure 4D and Supplementary Figure S6A). Total protein for C5aR was examined by immunoblot using antiC5aR antibody, and its comparative reduction in the *PODXL1*deficient cell was corroborated, using whole cell lysates, between

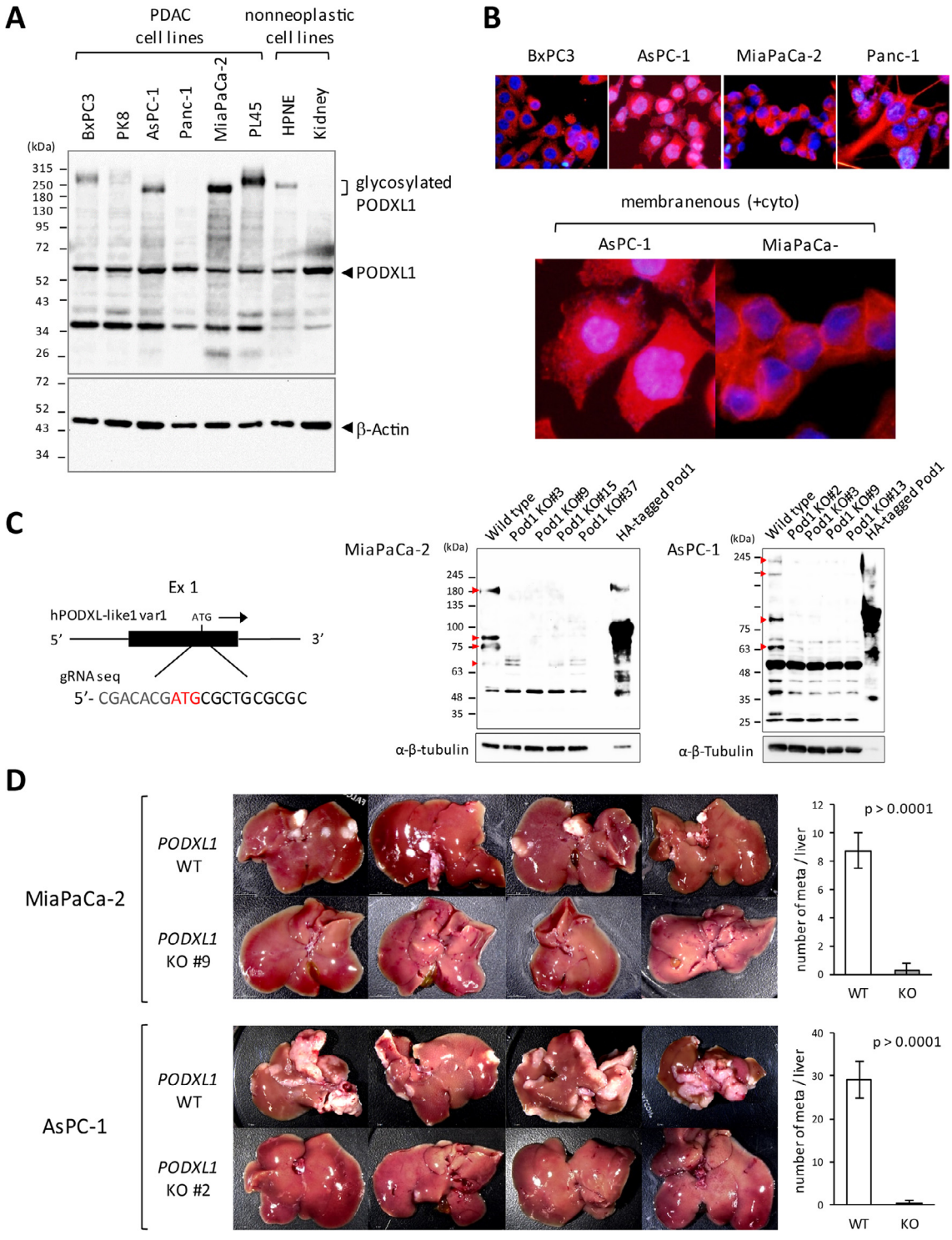

Figure 2. Loss of liver metastasis in the PODXL1-deficient PDAC cells *in vivo*. (A) endogenous PODXL1 expression in six PDAC lines (BxPC3, PK-8, Panc-1, MiaPaCa-2 and PL45), HPNE and kidney epithelial cells as a non-neoplastic by IB using anti-PODXL1 Ab. Note the glycosylated form of PODXL1 showed as supershifted. (B) Expression of PODXL1 detected by IF. Hyperview of AsPC-1 and MiaPaCa-2 showed expression of PODXL1 at the surface membrane as well as at the cytoplasm. (C) Schematic representation of the guide RNA design for the knockout, recognizing a part of the exon 3 (black box) within the PODXL1 genome (left). Confirmation of the KO clones of MiaPaCa-2 (#3, #9, #15, #37) and AsPC-1(#2, #3, #9, #13) by IB using anti-PODXL1 Ab. The 293T lysate transfected with HA-tagged ful-length PODXL1 variant 1 was used as a positive control. α--tubulin indicated the IB using anti-total tubulin Ab. (D) Development of liver metastasis 30 days after splenic injection of the *PODXL1*-WT or the KO cells in Balb/c nu/nu mice (n = 4 in each group). Attached Graphs showed average number of liver metastasis/mouse in MiaPaCa-2-injected or AsPC-1-injected mice (n = 4/each WT or KO group, means and s.d. of quadruplicate were shown).

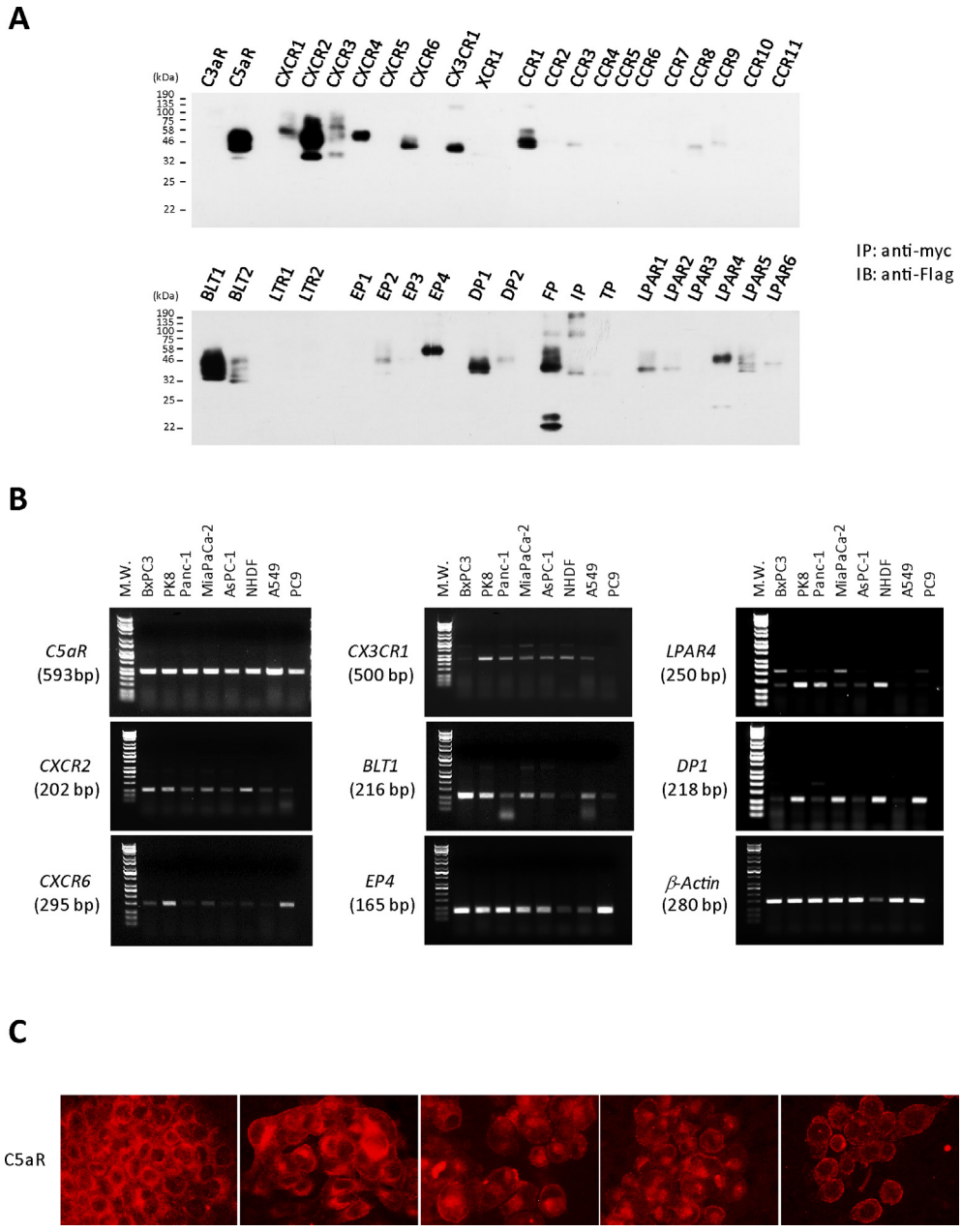

Figure 3. PODXL1 captures multiple chemokine receptors. (A) Panel screening of the forty chemokine receptors as a binding partner to PODXL1. Pull-down assay (IP) using anti-myc tag Ab for the lysates from the myc-tagged *PODXL1*-cotransfected 293T with each Flag-tagged chemokine receptor gene detected the specific binding partner to PODXL1. IB was performed by probing with anti-Flag Ab for the precipitates. (B) Expression of the each chemokine receptor that showed binding affinity to PODXL1 in Figure 3a was examined by RT-PCR among five PDAC lines, NHDF (fibroblast), A549 and PC9 (both lung adenocarcinoma lines). (C) IF using anti-C5aR Ab revealed membranous expression of C5aR on PDAC cells.

the WT cells and the KO cells, in MiaPaCa2 and AsPC1, respectively (Figure 4E, left panel). Furthermore, immunoblot of the cellular fraction revealed that the majority of C5aR was detected in the membrane fraction of PODXL1WT AsPC1 and MiaPaCa2 cells, respectively, while in the PODXL1KO cells the majority of C5aR was contained in the cytosol fraction (Figure 4E, right panel). These results implied that lack of PODXL1 might impair the protein stability and the functional localization of C5aR in PDAC cells. Given the aggregate findings, we examined whether the PODXL1C5aR interaction was involved in EMT of PDAC cells. Total cell lysates were prepared from each PDAC cell sample with or without C5a stimulation for 12 hours in the PODXL1WT and the KO phenotype of AsPC1 and MiaPaCa2. The sample from the C5atreated PODXL1WT cells showed marked reduction of ECadherin in contrast to an increase in Snail and Vimentin, whereas the KO phenotype displayed no significant quantitative fluctuations of these proteins (Figure 4F). The PODXL1C5aR/C5a axis was therefore demonstrated to be one of the critical pathways for triggering EMT of the PDAC cells.

Significance of C5aR/C5a axis for the PDAC metastasis in the presence of PODXL1 in vivo

With the specific interaction of PODXL1 and C5aR in PDAC cells thus confirmed, the biological impact of C5aR/C5a signaling for promot-

ing PDAC metastasis was examined using the experimental PDAC liver metastasis model in nude mice. Animals injected in the spleen with 1 10^6 of MiaPaCa2 cells were either treated three times, in total, with antiC5a neutralizing antibody (50 g/every 7 days), or with the same dose of goat IgG as a control following the schedule shown in Figure 5A. Thirty days after splenic injection of MiaPaCa2 cells, mice were freshly autopsied and examined for liver metastasis. Significant differences were thereby observed in number of metastatic tumor foci (representative histology for these metastatic tumors was shown in Supplementary Figure S6B) as shown in the stereoscopic image and the summarized graph, where the neutralizing antibodytreated mice were poorly showing in metastatic foci (Figure 5A). Thus, the activation of C5aR/C5a signal significantly contributed to liver metastasis formation of PDAC cells *in vivo*. Immunohistochemistry indicated that metastatic cancer cells were positive for C5a, C5aR, and PODXL1 (murine hepatocytes were also positive for C5a and C5aR), and immunofluorescence revealed the coexpression of

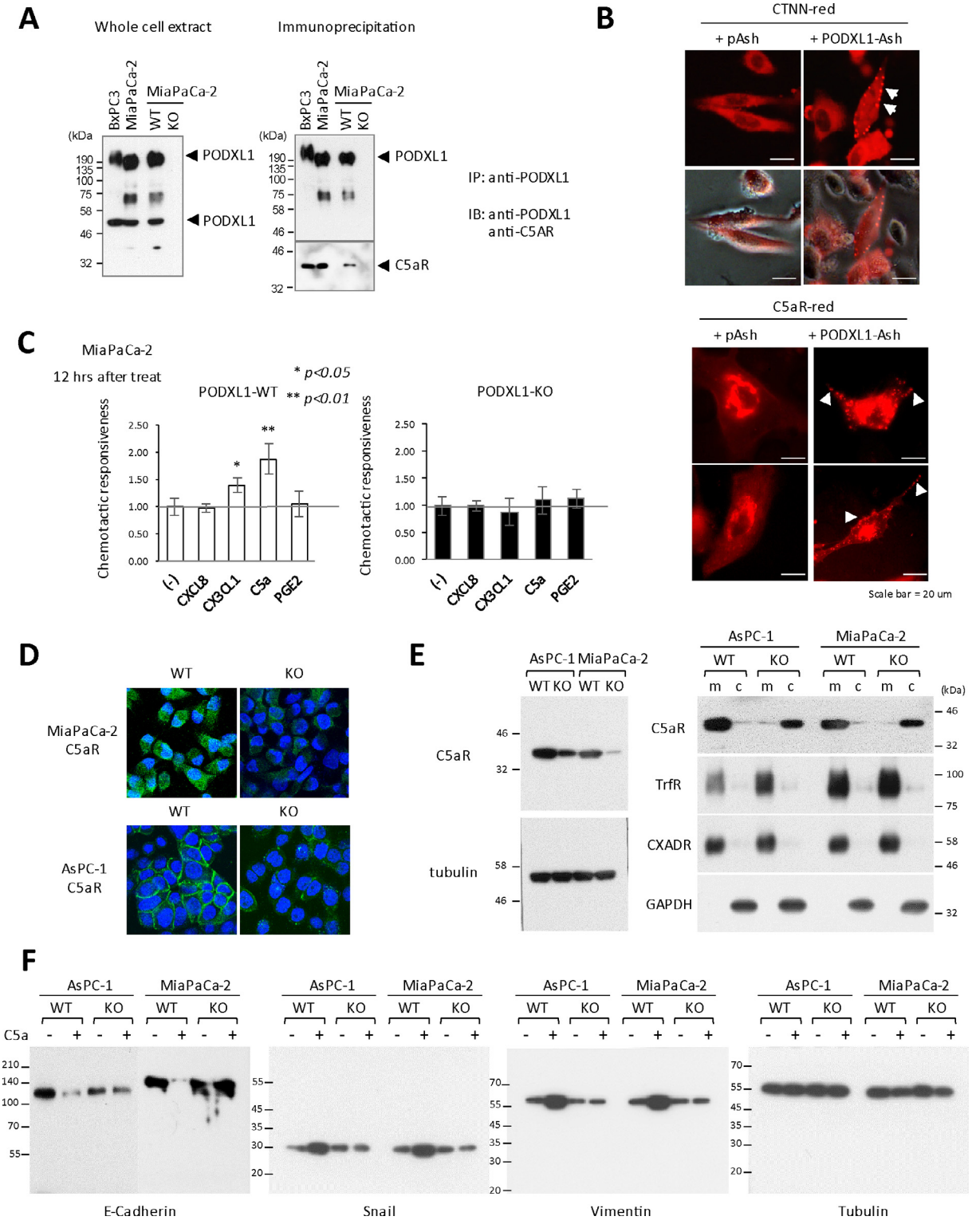

PODXL1 and Vimentin as an EMT marker on cancer cells at the metastatic foci (Figure 5B).

Detection of C5aR, C5a and PODXL1 in human PDAC patient primary tissues and liver metastatisis

Since the interaction between PODXL1 and C5aR/C5a axis was established in the mouse PDACxenografted model, we then investigated the endogenous expression of these molecules in human patient tissues. Strong C5aR expression was detected on the invasive nests of primary PDAC tissues as well as PODXL1 expression (Figure 6A), and the merged image of double immunofluorescence detecting PODXL1 and C5aR displayed a few double positive cells inside the invasive cancer nest with membranous colocalization (Figure 6B). In liver metastasis from the same PDAC patient, C5aR and PODXL1 were consistently expressed on the same individual cancer cells as well as in the primary site (Figure 6C), and C5a, as a ligand to C5aR, was strongly positive both on nonneoplastic hepatocytes (Figure 6D, upper panel) and metastatic PDAC cells (Figure 6D, lower panel, hyperview). C5aR expression was also maintained at the lymph nodal metastasis of PDAC (Supplementary Figure S7).

Discussion

In previous studies, expression of PODXL1 had been reported to reflect adverse prognosis for the patient with diverse cancer origins including breast, colorectal, gastric, and pancreatic adenocarcinoma [4,8–10,23]. Similarly, C5aR/C5a expression is known to correlate with clinical prognosis for various lineages of cancer [14,16,17]. Moreover, both PODXL1 signaling and C5aR/C5a signaling were proven molecularly to facilitate tumor cell invasion *in vitro* by activating specific kinases [13,24,25]. For example, PODXL1 triggers invasion by increased matrix metalloproteinases (MMP) 1 and 9 expression and increased activation of MAPK and PI3K activity through ezrin in breast cancer, and by elevating the soluble cat level/cat signaling through the p38 MAPK/GSK3 pathway in glioblastoma [10,12]. On the other hand, C5aR/C5a signaling was reported to raise the release of MMP from cancer cells – similarly to PODXL1 – to induce PI3K/AKT activation and inhibit p21/pp21 expression, and even to exhibit immunomodulatory effects in facilitating cancer metastasis by suppressing effector CD8(+) and CD4(+) Tcell responses [25–27]. Collectively, this information implicates the presently studied molecules as crucially determinant for metastasis, and for resultant poor prognosis, in a wide range of tumors. However, these molecules have also been reported as being independently significant in their biology. In this study, we found the direct molecular connection between PODXL1 and C5aR/C5a axis by demonstrating that PODXL1 is considered to be one of the important binding partner with C5aR, which stabilizes C5aR and recruits it to its functional site (cell membrane) on PDAC cells. Namely, PODXL1 is considered to be essential to activation of C5aR, leading to acquisition of cellular motility imparting invasive and metastatic properties to PDAC cells (Figure 6E). This novel finding may provide a clearcut explanation for the various earlier oncology studies on PODXL1 and C5aR/C5a, although further investigation is necessary for the detailed structure and function of the PODXL1C5aR complex, and for the mechanism of recruitment of the complex to the plasma membrane. Our experiments also revealed the multifunctional aspects of PODXL1 appearing to allow capture of multiple chemokine/cytokine receptors induced in the tumor microenvironment. We suggest that PODXL1 plays a central role in progression of diverse cancers by activating the soluble factors in response to their unique tumor microenvironment. This notion is supported by earlier reports that the glycosylated form of PODXL1, TRA160 antigen [22,28], was utilized as an important cellular marker for iPS cells to confirm their fullreprogramming status [29], reflecting a wide action permitting multipotent differentiation in response to diverse stimuli.

In a recent trend, multiple oncology studies in tumor medicine have emphasized the importance of the expulsion of cancer stem cells, as they are strongly resistant to known anticancer treatments and hence are sources for recurring malignancy. With that in mind it remains unclear whether PODXL1expressing tumors contain cancer stemphenotype cells, but the tumors may yet correlate highly with relapse and progression specifically due to the diverse function of PODXL1/TRA160 [30] in the microenvironment, as was demonstrated in this study. Our investigations, importantly, represent a framework for precision therapeutic control of the PODXL1expressing cancer cell, so as to overcome intractable malignancies such as PDACs.

Conclusions

In this study, we found novel crosstalk between the critical two tumor regulators, PODXL1 and C5aR, in pancreatic cancer (PDAC) which significantly contribute PDAC invasion/metastasis. Through their specific interaction, PDAC acquired accelerated cellular motility and caused aggressive metastasis which was corroborated by *in vivo* assays of xenografted model using *PODXL1*knockout PDAC cell in comparison with the wild type cell. Furthermore, PODXL1 may be multifunctional because it is capable of capturing various chemokine (cytokine) receptors, which suggests diverse role of PODXL1 in the tumor microenvironment.

Figure 4. PODXL1 accelerates PDAC cellular motility by activating C5aR with triggering EMT. (A) IP assay demonstrated PODXL1 specifically bound to C5aR. Endogenous expression of PODXL1 in the PODXL1-WT and the KO MiaPaCa-2 cells (left). Precipitates by anti-PODXL1 Ab probed with anti-C5aR Ab showed PODXL1-C5aR binding not in the KO cells but in the WT cells (right). (B) Visualizing the alteration of C5aR intracellular localization with or without PODXL1 by Fluoppi assay. Cellular localization of C5aR was examined on HeLa cotransfected with *PODXL1*-Ash and *C5aR*-red compared with the cells transfected with *C5aR*-red alone (lower panel). Correct system behavior was confirmed by the *PODXL1*-Ash + *CTTN*-red cotransfected cells (CTTN is a known binding partner of PODXL1) as a positive control (upper panel). Arrows indicated membrane localization of fluorescent dots. (C) Loss of the cellular motility in the *PODXL1*-KO cells treated with C5a by invasion assay (Boyden chamber assay). Accelerated motility of the *PODXL1*-WT MiaPaCa-2 in response to C5a (left), loss of the response in the *PODXL1*-KO cells (right). (D) Endogenous expression of C5aR in the *PODXL1*-WT and the KO cells of MiaPaCa-2 or AsPC-1 by IF using confocal-laser scanning microscope. (E) Decreased expression of C5aR in the *PODXL1*-KO PDAC cells in comparison with that in the WT cells (left). Marked shift of intracellular localization of C5aR demonstrated by IB for the extracts between membrane fraction and cytosolic fraction from the *PODXL1*-WT and *PODXL1*-KO PDAC cells (right). Transferrin receptor and CXADR were shown as positive control for membrane extract. (F) EMT triggered with C5a stimulation in the *PODXL1*-WT PDAC cells. Decreased expression of E-Cadherin, upregulation of Snail and Vimentin in the WT cells only when stimulated with C5a by IB. Tubulin was shown as a control.

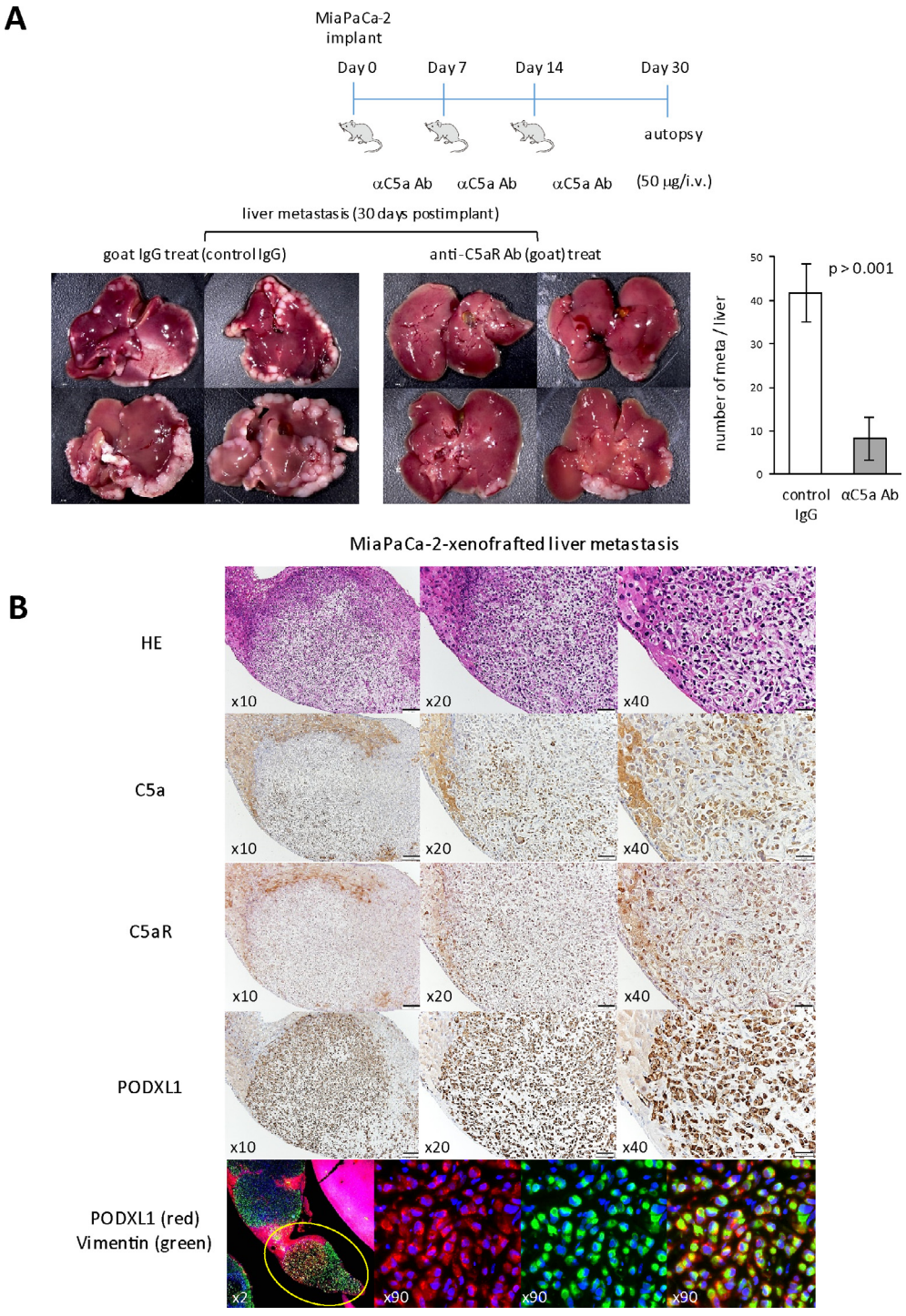

Figure 5. C5aR/C5a axis is essential to cause liver metastasis of MiaPaCa-2 *in vivo*. (A) Administration protocol of the C5a-neutralizing Ab (50 g/mouse/time) to the mice splenically injected with MiaPaCa-2 (1 10^6 cells). The mice splenically injected with MiaPaCa-2 had in total three intravenous injections of the Ab, once per week, and were autopsied on the Day 30 (upper panel). Development of liver metastasis of implanted MiaPaCa-2 cells with or without C5a Ab-treatment (lower panel). Attached Graphs showed average number of liver metastasis/mouse in the mice treated with control IgG or those treated with anti-C5a Ab (n = 4/each group, means and s.d. of quadruplicate were shown). (B) IHC analyses of the metastatic focus of MiaPaCa-2 in the mouse model. Liver isolated from the mice without treatment by anti-C5a Ab shown above was subjected to IHC analysis detecting C5a, C5aR, and PODXL1 expression on metastatic focus. The bottom panel showed coexpression of PODXL1 (red) and Vimentin (green) on an individual cancer cell by double IF.

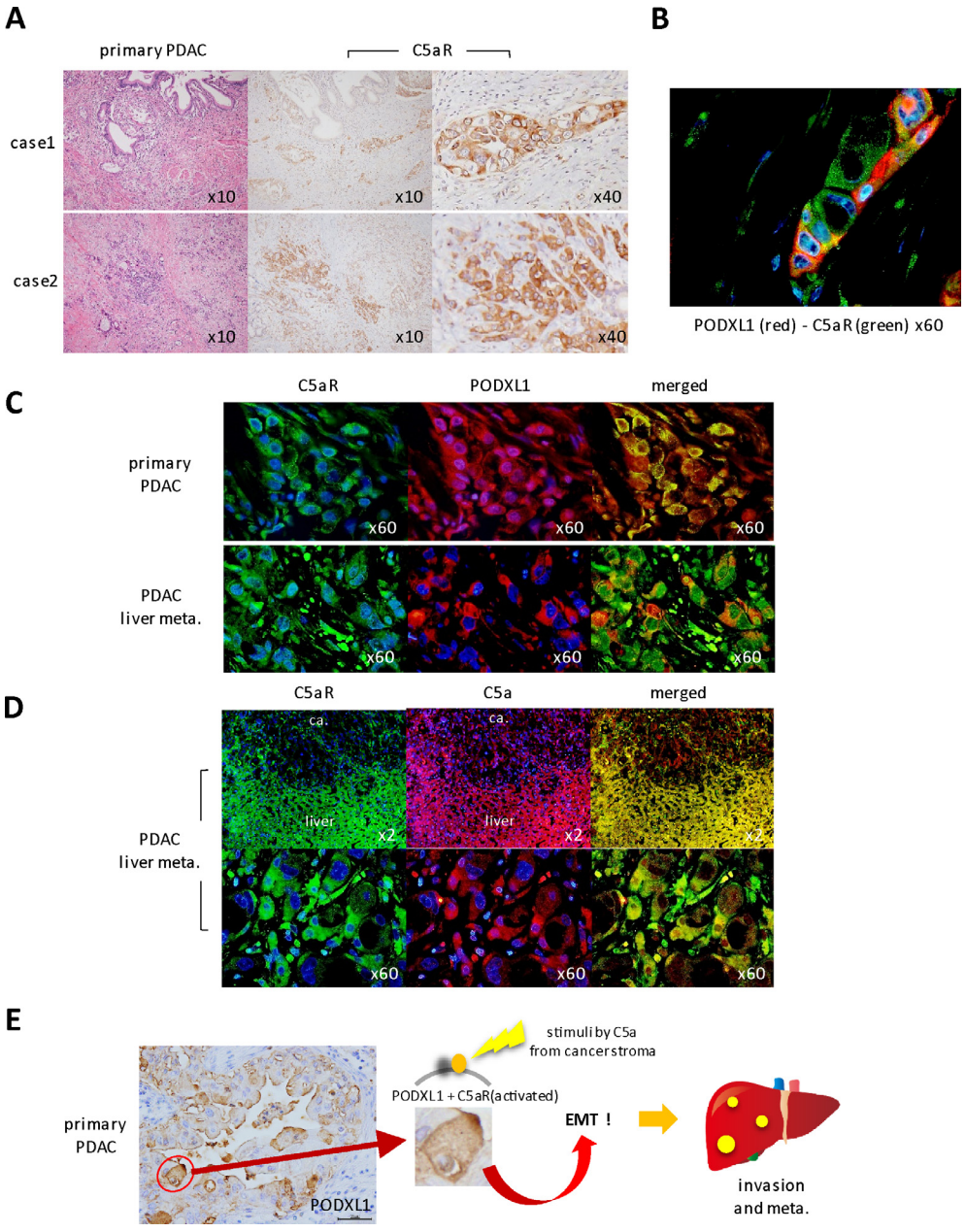

Figure 6. Endogenous expression of C5aR, PODXL1 and C5a on the PDAC patient tissues. (A) IHC staining of C5aR on the invasive nests of primary PDAC tissues (two cases of PDAC patients). (B) Double IF showed membranous colocalization of PODXL1 (red) and C5aR (green) on the cancer nest at the invasive front of human PDAC. (C) Coexpression of C5aR and PODXL1 on cancer cells of primary PDAC tissues and the liver metastasis of the same patient. (D) Coexpression of C5aR and C5a at the liver metastatic focus of the PDAC patient. Note that non-neoplastic hepatocytes are also positive for both. (E) Schematic representation of the specific interaction of PODXL1-C5aR/C5a axis in PDAC invasion/metastasis.

Acknowledgements

We thank Dr. K. Homma and T. Kawasaki (Dept. of Pathology, Niigata Cancer Center Hospital) for kindly supporting pathological materials, also Ms. N. Sumi and Ms. A. Ageishi for technical assistance and preparation of manuscript.

Funding

This study was supported by GrantinAid for Challenging Exploratory Research, Japan Society for the Promotion of Science (JSPS) KAKENHI Grant Number JP 16K15245 (E. Kondo).

Author contributions

E.K. conceived, designed, and supervised the study. K.S., H.I., S.M, W.S. and M.S. performed experiments. E.K. discussed the result with K.S., H.I., M.S. and wrote the manuscript.

Appendix A. Supplementary data

Supplementary data to this article can be found online at https://doi.org/10.1016/j.neo.2019.09.003.

References

1. Neoptolemos JP, Palmer DH, Ghaneh P, Psarelli EE, Valle JW, Halloran CM, Faluyi O, O'Reilly DA, Cunningham D, Wadsley J, etal. Comparison of adjuvant gemcitabine and capecitabine with gemcitabine monotherapy in patients with resected pancreatic cancer (ESPAC-4): a multicentre, open-label, randomised, phase 3 trial. *Lancet* 2017;**389**(10073):1011–24.
2. Neoptolemos JP, Kleeff J, Michl P, Costello E, Greenhalf W, Palmer DH. Therapeutic developments in pancreatic cancer: current and future perspectives. *Nat Rev Gastroenterol Hepatol* 2018;**15**(16):333–48.
3. Horvat R, Hovorka A, Dekan G, Poczewski H, Kerjaschki D. Endothelial cell membranes contain podocalyxin–the major sialoprotein of visceral glomerular epithelial cells. *J Cell Biol* 1986;**102**:484–91.
4. Somasiri A, Nielsen JS, Makretsov N, McCoy ML, Prentice L, Gilks CB, Chia KA, Gelmon KA, Kershaw DB, Huntsman DG, etal. Overexpression of the anti-adhesin podocalyxin is an independent predictor of breast cancer progression. *Cancer Res* 2004;**64**:5068–73.
5. Doyonnas R, Nielsen JS, Chelliah S, Drew E, Hara T, Miyajima A, McNagny KM. Podocalyxin is a CD34-related marker of murine hematopoietic stem cells and embryonic erythroid cells. *Blood* 2005;**105**:4170–8.
6. Bhattacharya B, Miura T, Brandenberger R, Mejido J, Luo Y, Yang AX, Joshi I, Ginis I, Thies RS, Amit M, etal. Gene expression in human embryonic stem cell lines: unique molecular signature. *Blood* 2004;**103**:2956–64.
7. Richards M, Tan SP, Tan JH, Chan WK, Bongso A. The transcriptome profile of human embryonic stem cells as defined by SAGE. *Stem Cells* 2004;**22**:51–64
8. Kaprio T, Fermr C, Hagstrm J, Mustonen H, Bckelman C, Nilsson O, Haglund C. Podocalyxin is a marker of poor prognosis in colorectal cancer. *BMC Cancer* 2014;**14**:493.
9. Laitinen A, Bckelman C, Hagstrm J, Kokkola A, Fermr C, Nilsson O, Haglund C. Podocalyxin as a prognostic marker in gastric cancer. *PLoS ONE* 2015;**10** e0145079.
10. Saukkonen K, Hagstrm J, Mustonen H, Juuti A, Nordling S, Fermr C, Nilsson H, Seppnen H, Haglund C. Podocalyxin is a marker of poor prognosis in pancreatic ductal adenocarcinoma. *PLoS One* 2015;**10** e0129012.
11. Lin CW, Sun MS, Liao MY, Chung CH, Chi YH, Chiou LT, Yu J, Lou KL, Wu HC. Podocalyxin-like 1 promotes invadopodia formation and metastasis through activation of Rac1/Cdc42/cortactin signaling in breast cancer cells. *Carcinogenesis* 2014;**35**:2425–35.
12. Sizemore S, Cicek M, Sizemore N, Ng KP, Casey G. Podocalyxin increases the aggressive phenotype of breast and prostate cancer cells in vitro through its interaction with ezrin. *Cancer Res* 2007;**67**:6183–91.
13. Graves ML, Cipollone JA, Austin P, Bell EM, Nielsen JS, Gilks CB, McNagny CD, Roskelley CD. The cell surface mucin podocalyxin regulates collective breast tumor budding. *Breast Can Res* 2016;**18**:11.
14. Imamura T, Yamamoto-Ibusuki M, Sueta A, Kubo T, Irie A, Kikuchi K, Kariu H, Iwase H. Influence of the C5a–C5a receptor system on breast cancer progression and patient prognosis. *Breast Cancer* 2016;**23**:876–85.
15. Kaida T, Nitta H, Kitano Y, Yamamura K, Arima K, Izumi D, Higashi T, Kurashige J, Imai K, Hayashi H, etal. C5a receptor (CD88) promotes motility and invasiveness of gastric cancer by activating RhoA. *Oncotarget* 2016;**7**:84798–809.
16. Gua J, Dinga JY, Lu CL, Lin ZW, Chu YW, Zhao GY, Guo J, Ge D. Overexpression of CD88 predicts poor prognosis in non-small-cell lung cancer. *Lung Cancer* 2013;**81**:259–65.
17. Wada Y, Maeda Y, Kubo T, Kikuchi K, Eto M, Imamura T. C5a receptor expression is associated with poor prognosis in urothelial cell carcinoma patients treated with radical cystectomy or nephroureterectomy. *Oncol Lett* 2016;**12**:3995–4000.
18. Sakaguchi M, Watanabe M, Kinoshita R, Kaku H, Ueki H, Futami J, Murata Y, Inoue Y, Li SA, Huang P, etal. Dramatic increase in expression of a transgene by insertion of promoters downstream of the cargo gene. *Mol Biotechnol* 2014;**56**:621–30.
19. Koyano F, Okatsu K, Kosako H, Tamura Y, Go E, Kimura M, Kimura Y, Tsuchiya H, Yoshihara H, Hirokawa T, etal. Ubiquitin is phosphorylated by PINK1 to activate parkin. *Nature* 2014;**510**:162–6.
20. Yamano K, Queliconi BB, Koyano F, Saeki Y, Hirokawa T, Tanaka K, Matsuda N. Site-specific interaction mapping of phosphorylated ubiquitin to uncover parkin activation. *J Biol Chem* 2015;**290**:25199–211.
21. Ney JT, Zhou H, Sipos B, Bttner R, Chen X, Klppel G, Gtgemann I. Podocalyxin-like protein 1 expression is useful to differentiate pancreatic ductal adenocarcinomas from adenocarcinomas of the biliary and gastrointestinal tracts. *Hum Pathol* 2007;**38**:359–64.
22. Schopperle WM, DeWolf WC. The TRA-1-60 and TRA-1-81 human pluripotent stem cell markers are expressed on podocalyxinin embryonal carcinoma. *Stem Cells* 2007;**25**:723–30.
23. Heby M, Elebro J, Nodin B, Jirstrm K, Eberhard J. Prognostic and predictive significance of podocalyxin-like protein expression in pancreatic and periampullary adenocarcinoma. *BMC Clin Pathol* 2015;**15**:10.
24. Frse J, Chen MB, Hebron KE, Reinhardt F, Hajal C, Zijlstra A, Kamm RD, Weinberg RA. Epithelial-mesenchymal transition induces podocalyxin to promote extravasation via ezrin signaling. *Cell Rep* 2018;**24**:962–72.
25. Vadrevu SK, Chintala NK, Sharma SK, Sharma P, Cleveland C, Riediger L, Manne S, Fairlie DP, Gorczyca W, Almanza O, etal. Complement c5a receptor facilitates cancer metastasis by altering T-cell responses in the metastatic niche. *Cancer Res* 2014;**74**:3454–65.
26. Nitta H, Wada Y, Kawano Y, Murakami Y, Irie A, Taniguchi K, Kikuchi K, Yamada G, Suzuki K, Honda J, etal. Enhancement of human cancer cell motility and invasiveness by anaphylatoxin C5a via aberrantly expressed C5a receptor (CD88). *Clin Cancer Res* 2013;**19**:2004–13.
27. Chen J, Li GQ, Zhang L, Tang M, Gao X, Xu GL, Wu YZ. Complement C5a/C5aR pathway potentiates the pathogenesis of gastric cancer by down-regulating p21 expression. *Cancer Lett* 2018;**412**:30–6.
28. Toyoda H, Nagai Y, Kojima A, Kinoshita-Toyoda A. Podocalyxin as a major pluripotent marker and novel keratan sulfate proteoglycan in human embryonic and induced pluripotent stem cells. *Glycoconj J* 2017;**34**:817–23.
29. Chan EM, Ratanasirintrawoot S, Park IH, Manos PD, Loh YH, Huo H, Miller O, Hartung O, Rho J, Ince TA, etal. Live cell imaging distinguishes bona fide human iPS cells from partially reprogrammed cells. *Nat Biotechnol* 2009;**27**:1033–7.
30. Takata K, Saito K, Maruyama S, Miyata-Tanaka T, Iioka H, Okuda S, Ling Y, Karube K, Miki Y, Maeda Y, etal. Identification of TRA-1-60-positive cells as a potent refractory population in follicular lymphomas. *Cancer Sci* 2019;**110**:443–57.